

## A new weighted Lindley distribution with application

A. Asgharzadeh<sup>a</sup>, Hassan S. Bakouch<sup>b,c</sup>, S. Nadarajah<sup>d</sup> and F. Sharafi<sup>a</sup>

<sup>a</sup>University of Mazandaran

<sup>b</sup>Tanta University

<sup>c</sup>King Abdulaziz University

<sup>d</sup>University of Manchester

**Abstract.** The Lindley distribution has been generalized by many authors in recent years. Here, we introduce a new generalization that provides better fits than the Lindley distribution and all of its known generalizations. The distribution contains Lindley and weighted Lindley (Ghitany et al. (*Math. Comput. Simulation* **81** (2011) 1190–1201)) distributions as special cases. Also, the distribution can be represented as a mixture of weighted exponential (Gupta and Kundu (*Statistics* **43** (2009) 621–634)) and weighted gamma distributions, and as a negative mixture of Lindley distributions with different parameters. Various properties of the distribution (including quantiles, moments, moment generating function, hazard rate function, mean residual lifetime, Lorenz curve, Gini index, Rényi entropy and Mathai–Haubold entropy) are derived. Maximum likelihood estimators of the distribution parameters are derived and their behavior is assessed via simulation. Fisher’s information matrix and asymptotic confidence intervals for the distribution parameters are given. Finally, a real data application is presented.

### 1 Introduction

Weighted distributions are useful for better understanding of standard distributions and can extend distributions by adding flexibility. Also, truncated and damaged observations can be analyzed using weighted distributions. Azzalini (1985) proposed a new method for introducing a skewness parameter to the normal distribution based on a weighted function and obtained the skew-normal distribution. Azzalini’s idea has been applied to other symmetric distributions and many skew-symmetric distributions have been developed; for example, the skew-logistic distribution due to Nadarajah (2009). Gupta and Kundu (2009) used a similar approach to Azzalini for introducing a skewness parameter to the exponential distribution and constructed a new class of weighted exponential distributions, which are generalizations of the exponential distribution and are similar to the Weibull, gamma and exponentiated exponential distributions. They showed that the weighted exponential distribution can be used to analyze positively skewed data, like the distributions mentioned above, and data coming from hidden truncated models.

---

*Key words and phrases.* Estimation, Gini index, skewness, weighted distributions.  
Received April 2014; accepted June 2014.

Shakhatreh (2012) proposed a new class of two-parameter weighted exponential distributions which generalizes the class of weighted exponential distributions.

The aim of this paper is to introduce a skewness parameter to the Lindley distribution using a similar idea to Gupta and Kundu (2009) and to obtain a new weighted Lindley (NWL) distribution. The Lindley distribution was originally introduced by Lindley (1958) in the context of Bayesian statistics. It has the probability density function (p.d.f.)

$$f(x, \lambda) = \frac{\lambda^2}{1 + \lambda}(1 + x)e^{-\lambda x} \quad (1)$$

for  $x > 0$  and  $\lambda > 0$ . Ghitany et al. (2008) investigated properties of the Lindley distribution with application and outlined that the Lindley distribution is a better model than one based on the exponential distribution. Ghitany et al. (2013) showed that the Lindley distribution can be written as a mixture of an exponential distribution and a gamma distribution with shape parameter 2.

Many generalizations of the Lindley distribution have been proposed in recent years. The generalizations that we are aware of are: the generalized Lindley (GL) distribution due to Zakerzadeh and Dolati (2009) with the p.d.f.

$$f(x) = \frac{\theta^2(\theta x)^{\alpha-1}(\alpha + \gamma x)e^{-\theta x}}{(\gamma + \theta)\Gamma(\alpha + 1)} \quad (2)$$

for  $x > 0$ ,  $\alpha > 0$ ,  $\theta > 0$  and  $\gamma > 0$ ; the weighted Lindley (WEL) distribution due to Ghitany et al. (2011) with the p.d.f.

$$f(x) = \frac{\theta^{c+1}}{(\theta + c)\Gamma(c)}x^{c-1}(1 + x)e^{-\theta x} \quad (3)$$

for  $x > 0$ ,  $c > 0$  and  $\theta > 0$ ; the extended Lindley (EL) distribution due to Bakouch et al. (2012) with the p.d.f.

$$f(x) = \frac{\lambda(1 + \lambda + \lambda x)^{\alpha-1}}{(1 + \lambda)^\alpha}[\beta(1 + \lambda + \lambda x)(\lambda x)^{\beta-1} - \alpha]e^{-(\lambda x)^\beta} \quad (4)$$

for  $x > 0$ ,  $\alpha \in (-\infty, 0) \cup \{0, 1\}$ ,  $\beta > 0$  and  $\lambda > 0$ ; the exponential Poisson Lindley (EPL) distribution due to Barreto-Souza and Bakouch (2013) with the p.d.f.

$$f(x) = \frac{\beta\theta^2(1 + \theta)^2e^{-\beta x}(3 + \theta - e^{-\beta x})}{(1 + 3\theta + \theta^2)(1 + \theta - e^{-\beta x})^3} \quad (5)$$

for  $x > 0$ ,  $\theta > 0$  and  $\beta > 0$ ; the power Lindley (PL) distribution due to Ghitany et al. (2013) with the p.d.f.

$$f(x) = \frac{\alpha\beta^2}{\beta + 1}(1 + x^\alpha)x^{\alpha-1}e^{-\beta x^\alpha} \quad (6)$$

for  $x > 0$ ,  $\alpha > 0$  and  $\beta > 0$ ; the Weibull Lindley (WL) distribution due to [Asgharzadeh et al. \(2014b\)](#) with the p.d.f.

$$f(x) = \frac{1}{1 + \lambda} [\alpha \lambda (\beta x)^\alpha + \alpha \beta (1 + \lambda) (\beta x)^{\alpha-1} + \lambda^2 (1 + x)] e^{-\lambda x - (\beta x)^\alpha} \quad (7)$$

for  $x > 0$ ,  $\alpha > 0$ ,  $\beta > 0$  and  $\lambda > 0$ ; the generalized inverse Lindely (GIL) distribution due to [Asgharzadeh et al. \(2014a\)](#) with the p.d.f.

$$f(x) = \frac{\alpha \lambda^2}{\lambda + 1} (1 + x^{-\alpha}) x^{-\alpha-1} e^{-\lambda x^{-\alpha}} \quad (8)$$

for  $x > 0$ ,  $\alpha > 0$  and  $\lambda > 0$ .

However, there are situations in which the Lindley distribution and all of its generalizations may not be suitable from a theoretical or an applied point of view. Here, we describe such a situation. We introduce a two-parameter distribution that provides better fits than the Lindley distribution and all of its generalizations for at least one real data set (in spite of the fact that three known generalizations have three parameters each). It is a two-parameter generalization of the Lindley distribution referred to as the NWL distribution. Some other motivation for the NWL distribution are that it (i) extends the skewness of the Lindley distribution from  $[\sqrt{2}, 2]$  to  $[\frac{2}{\sqrt{3}}, 3]$ ; (ii) contains the two-parameter weighted Lindley distribution due to [Ghitany et al. \(2011\)](#) and the Lindley distribution as particular cases; (iii) takes the form of a mixture of weighted exponential and weighted gamma distributions; (iv) takes the form of a negative mixture of the Lindley distribution with different parameters; (v) has the hazard rate function bounded; (vi) gives realistic values for the Gini index; (vii) gives closed form expressions for the Fisher information matrix.

A final motivation is that the proposed distribution exhibits only unimodal p.d.f.s and increasing hazard rates. The latter may seem unrealistic at first sight. But there are many situations where only increasing hazard rates are used or observed: [Milkie and Perakis \(2004\)](#) state “The results of the failure data analysis on the Reliance class propulsion system casualties support a lifecycle with an increasing failure rate. The original hypothesis that the evidence would indicate either a constant or decreasing failure rate as operating hours increase appears false”; [Maeda and Nishikawa \(2006\)](#) state “Ruling parties in presidential systems face an increasing hazard rate in their survival”; [Woosley and Cossman \(2007\)](#) observe that drugs during clinical development have increasing hazard rates; [Saidane et al. \(2011\)](#) suppose that the demand interval in spare parts inventory systems has increasing hazard rates; [Tsarouhas and Arvanitoyannis \(2010\)](#) show that machines of the bread production display increasing hazard rates; [Koutras \(2011\)](#) finds that software degradation times have increasing hazard rates; [Lai \(2013\)](#) investigates the optimum number of minimal repairs for systems under increasing hazard rates; and so on.

The real data set that we consider in this paper is taken from [Ugarte et al. \(2008\)](#):

1501.82	6989.43	2424.02	4150.29	8693.35	2643.77
13148.37	6149.39	23587.21	7248.37	4788.22	6009.51
5349.65	5741.32	7065.81	7261.37	2358.42	10357.88
2499.05	3022.90	4234.86	4482.03	6363.71	3329.91
8740.47	3664.95	4515.97	8497.71	4569.89	8069.63
7366.79	1525.41	3363.02	2420.57	3576.74	3708.05
5819.12	5479.38				

These data are carbon retained by leaves measured in kilogram/hectare for thirty eight different plots of mountainous regions of Navarra (Spain), depending on the forest classification: areas with ninety percent or more beech trees (*Fagus Sylvatica*) are labeled monospecific, while areas with many species of trees are labeled multispecific. These data have a sample skewness of 2.520, so the data cannot be adequately modeled by the Lindley distribution in (1). We shall refer to the data as carbon data.

A smoothed nonparametric p.d.f. and a smoothed nonparametric hazard rate function of the carbon data are shown in Figure 1. We can see that the p.d.f. is unimodal and that the hazard rate is increasing. So, the proposed distribution is suitable for modeling the carbon data.

The rest of this paper is organized as follows. Various mathematical properties of the NWL distribution (like quantiles, moments, moment generating function, hazard rate function, mean residual lifetime, Lorenz curve, Gini index, Rényi entropy and Mathai–Haubold entropy) are derived in Sections 2 and 3. Inference with simulation and a real data application for the NWL distribution are discussed in Section 4.

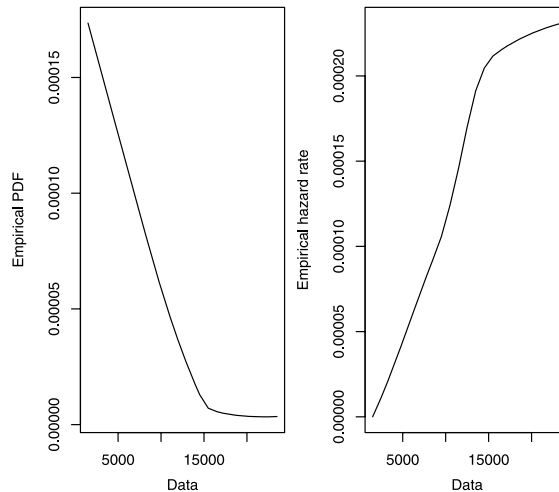


**Figure 1** Smoothed nonparametric p.d.f. and hazard rate of the carbon data.

## 2 The distribution and some properties

In this section, we define the NWL distribution and study shape properties of its p.d.f. The study of shapes is useful to determine if a data set can be modeled by the NWL distribution.

**Definition 1.** A random variable  $X$  follows the NWL distribution with parameters  $\lambda > 0$  and  $\alpha > 0$  if it has the p.d.f.

$$f(x) = \frac{\lambda^2(1+\alpha)^2}{\alpha\lambda(1+\alpha) + \alpha(2+\alpha)}(1+x)(1-e^{-\lambda\alpha x})e^{-\lambda x} \quad (9)$$

for  $x > 0$ . The corresponding cumulative distribution function is

$$F(x) = 1 - \frac{e^{-\lambda x}\{(1+\alpha)^2(1+\lambda+\lambda x) - [\lambda(1+\alpha)(1+x) + 1]e^{-\alpha\lambda x}\}}{\alpha\lambda(1+\alpha) + \alpha(2+\alpha)} \quad (10)$$

for  $x > 0$ .

### Remarks.

1. The Lindley distribution is the particular case of the NWL distribution for  $\alpha \rightarrow +\infty$ .
2. The limit of (9) as  $\alpha \rightarrow 0$  is

$$f(x) = \frac{\lambda^3}{2+\lambda}x(1+x)e^{-\lambda x},$$

which is the p.d.f. of the weighted Lindley distribution due to [Ghitany et al. \(2011\)](#) with parameters 2 and  $\lambda$ .

3. The NWL distribution can be expressed as a mixture of the weighted exponential distribution with parameters  $\lambda$  and  $\alpha$  and the weighted gamma distribution with parameters 2,  $\lambda$  and  $\alpha$ . That is,

$$f(x) = p\frac{\lambda(1+\alpha)}{\alpha}e^{-\lambda x}(1-e^{-\lambda\alpha x}) + (1-p)\frac{\lambda^2(1+\alpha)^2}{\alpha(2+\alpha)}xe^{-\lambda x}(1-e^{-\lambda\alpha x}),$$

where  $p = \frac{\lambda(1+\alpha)}{\lambda(1+\alpha)+2+\alpha}$ .

4. The NWL distribution can be expressed as a negative mixture of the Lindley distribution with parameter  $\lambda$  and the Lindley distribution with parameter  $\lambda(1+\alpha)$ . That is,

$$f(x) = p\frac{\lambda^2}{1+\lambda}(1+x)e^{-\lambda x} + (1-p)\frac{\lambda^2(1+\alpha)^2}{1+\lambda+\lambda\alpha}(1+x)e^{-\lambda(1+\alpha)x},$$

where  $p = \frac{(1+\alpha)^2(1+\lambda)}{\alpha\lambda(1+\alpha)+\alpha(2+\alpha)}$ .

The following proposition derives the analytic shapes of the p.d.f.  $f(x)$ . It shows that the p.d.f. is log-concave. Log-concavity is an important property. Among other areas it has applications in white noise analysis (Asai et al., 2001) and stochastic optimization (Ninh and Prekopa, 2013).

**Proposition 1.** *The p.d.f.  $f(x)$  of the NWL distribution is log-concave and unimodal.*

**Proof.** The second derivative of  $\log f(x)$  is

$$\frac{d^2 \log f(x)}{dx^2} = -\frac{1}{(1+x)^2} - \frac{\alpha^2 \lambda^2 \exp(-\alpha \lambda x)}{[1 - \exp(-\alpha \lambda x)]^2}.$$

We see that  $\log f(x)$  is concave for all  $\lambda$  and  $\alpha$ . So,  $f(x)$  is log-concave and unimodal.  $\square$

**Corollary 1.** *Solving the equation  $\frac{d \log f(x)}{dx} = 0$ , the mode  $M$  of the NWL distribution is the root of*

$$M = \frac{1}{\lambda} \{e^{-\alpha \lambda M} [-1 + (1 + M)(\lambda + \alpha \lambda)] + 1 - \lambda\}.$$

*In the limiting case  $\alpha \rightarrow +\infty$ , we find that  $M = \frac{1-\lambda}{\lambda}$ , the mode of the Lindley distribution.*

Note that  $f(0) = 0$ ,  $f(+\infty) = 0$ ,

$$f(x) \sim \frac{\lambda^3(1+\alpha)^2}{\lambda(1+\alpha) + \alpha(2+\alpha)} x$$

as  $x \rightarrow 0$  and

$$f(x) \sim \frac{\lambda^2(1+\alpha)^2}{\alpha\lambda(1+\alpha) + \alpha(2+\alpha)} x e^{-\lambda x}$$

as  $x \rightarrow +\infty$ . The lower tail of the NWL p.d.f. is polynomial while its upper tail is exponential. Figure 2 plots  $f(x)$  for different values of  $\alpha$  and  $\lambda$ . We see that the magnitude of the mode increases with increasing values of  $\alpha$  and  $\lambda$ . The location of the mode decreases with increasing values of  $\alpha$  and  $\lambda$ .

### 3 Statistical and reliability measures

In this section, we give some important statistical and reliability measures for the NWL distribution like quantiles, moment generating function, moments, hazard rate and mean residual life functions, Lorenz curve, Gini index, Rényi entropy and Mathai–Haubold entropy.

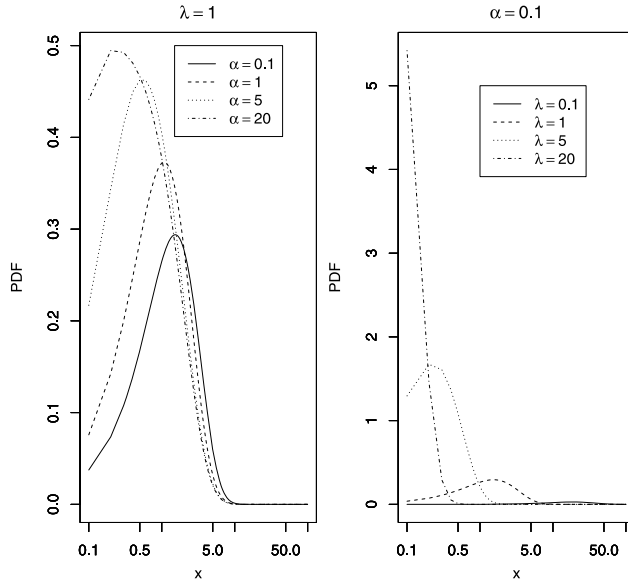


**Figure 2** Probability density function of the NWL distribution. The  $x$  axes are in log scale.

### 3.1 Quantiles, moment generating function and moments

Quantiles are fundamental for estimation (for example, quantile estimators) and simulation. Moment properties are fundamental for any distribution. For instance, the first four moments can be used to describe any data fairly well. Moments are also useful for estimation.

**Proposition 2.** The  $p$ th quantile  $x_p$  of the NWL distribution defined by  $F(x_p) = p$  is the root of the equation

$$x_p = \frac{1}{\lambda} \log \left[ \frac{(1 + \alpha)^2(1 + \lambda + \lambda x_p) - e^{-\alpha \lambda x_p} [\lambda(1 + \alpha)(x_p + 1) + 1]}{\alpha(1 - p)[\lambda(1 + \alpha) + 2 + \alpha]} \right]. \quad (11)$$

Note that  $x_p$  can be used to generate NWL random variates.

**Proposition 3.** Let  $X$  denote a NWL random variable. Its moment generating function and  $r$ th moment about the origin are

$$E(e^{tX}) = \frac{\lambda^2(1 + \alpha)^2}{\alpha\lambda(1 + \alpha) + \alpha(2 + \alpha)} \left\{ \frac{\lambda - t + 1}{(\lambda - t)^2} - \frac{\lambda(1 + \alpha) - t + 1}{[\lambda(1 + \alpha) - t]^2} \right\}$$

and

$$\mu'_r = E(X^r) = \frac{r![(1 + \alpha)^{r+2}(\lambda + r + 1) - \lambda(1 + \alpha) - r - 1]}{\lambda^r(1 + \alpha)^r[\alpha\lambda(1 + \alpha) + \alpha(2 + \alpha)]},$$

respectively. In particular,

$$E(X) = \mu = \frac{(1 + \alpha)^3(\lambda + 2) - (1 + \alpha)\lambda - 2}{\lambda(1 + \alpha)[\lambda\alpha(1 + \alpha) + \alpha(2 + \alpha)]},$$

$$E(X^2) = 2 \frac{(1 + \alpha)^4(\lambda + 3) - (1 + \alpha)\lambda - 3}{\lambda^2(1 + \alpha)^2[\lambda\alpha(1 + \alpha) + \alpha(2 + \alpha)]}$$

and

$$\text{Var}(X) = \frac{a_2(\alpha)\lambda^2 + a_1(\alpha)\lambda + a_0(\alpha)}{\lambda^2(1 + \alpha)^2[\lambda(1 + \alpha) + 2 + \alpha]^2},$$

where  $a_2(\alpha) = (1 + \alpha)^2(2 + 2\alpha + \alpha^2)$ ,  $a_1(\alpha) = 2(1 + \alpha)(2 + \alpha)(3 + 3\alpha + 2\alpha^2)$  and  $a_0(\alpha) = 2(6 + 12\alpha + 12\alpha^2 + 6\alpha^3 + \alpha^4)$ . Note that  $\lim_{\lambda \rightarrow 0} \text{Var}(X) = (2 + 2\alpha + \alpha^2)/(2 + \alpha)^2 > 0$  and  $a_2(\alpha)\lambda^2 + a_1(\alpha)\lambda + a_0(\alpha)$  has a minimum at  $-a_1(\alpha)/a_0(\alpha) < 0$ .

**Remark 1.** The central moments of  $X$  are  $\mu_r = E(X - \mu)^r = \sum_{k=0}^r \binom{r}{k} \times \mu'_k(-\mu)^{r-k}$ . The skewness and kurtosis of  $X$  can be obtained using the formulas  $\text{skewness}(X) = \mu_3/\sigma^3$  and  $\text{kurtosis}(x) = \mu_4/\sigma^4$ , where  $\sigma^2 = \text{Var}(X)$ .

Figure 3 plots the mean, variance, skewness and kurtosis of the NWL distribution. We see that the mean and variance are decreasing as both  $\alpha$  and  $\lambda$  increase. On the other hand, the skewness and kurtosis are increasing as both  $\alpha$  and  $\lambda$  increase. We can also see that the NWL distribution extends the skewness of the Lindley distribution from  $[\sqrt{2}, 2]$  to  $[2/\sqrt{3}, 3]$ . The increase in the range is modest however.

The range  $[2/\sqrt{3}, 3]$  was determined numerically by computing the skewness over  $\alpha = 0.01, 0.02, \dots, 100$  and  $\lambda = 0.01, 0.02, \dots, 100$ . We have no analytical proof that the skewness belongs to  $[2/\sqrt{3}, 3]$ . This is a possible future work.

Another measure of skewness is MacGillivray's skewness function (MacGillivray, 1986) defined by

$$\rho_M(p) = \frac{\rho_M^{(1)}}{\rho_M^{(2)}} = \frac{x_p + x_{1-p} - 2x_{0.5}}{x_p - x_{1-p}}$$

for  $0 < p < 1$ . From (11), we obtain

$$\begin{aligned} \rho_M^{(1)} = & \log \left\{ [(1 + \alpha)^2(1 + \lambda + \lambda x_p) - e^{-\alpha \lambda x_p}(\lambda(1 + \alpha)(x_p + 1) + 1)] \right. \\ & \times [(1 + \alpha)^2(1 + \lambda + \lambda x_{1-p}) - e^{-\alpha \lambda x_{1-p}}(\lambda(1 + \alpha)(x_{1-p} + 1) + 1)] \\ & \left. \times \left[ \frac{\alpha}{2}(\lambda(1 + \alpha) + 2 + \alpha) \right]^2 \right\} \\ & - \log \{ [\alpha(1 - p)(\lambda(1 + \alpha) + 2 + \alpha)][\alpha p(\lambda(1 + \alpha) + 2 + \alpha)] \\ & \times [(1 + \alpha)^2(1 + \lambda + \lambda x_{0.5}) - e^{-\alpha \lambda x_{0.5}}(\lambda(1 + \alpha)(x_{0.5} + 1) + 1)]^2 \} \end{aligned}$$

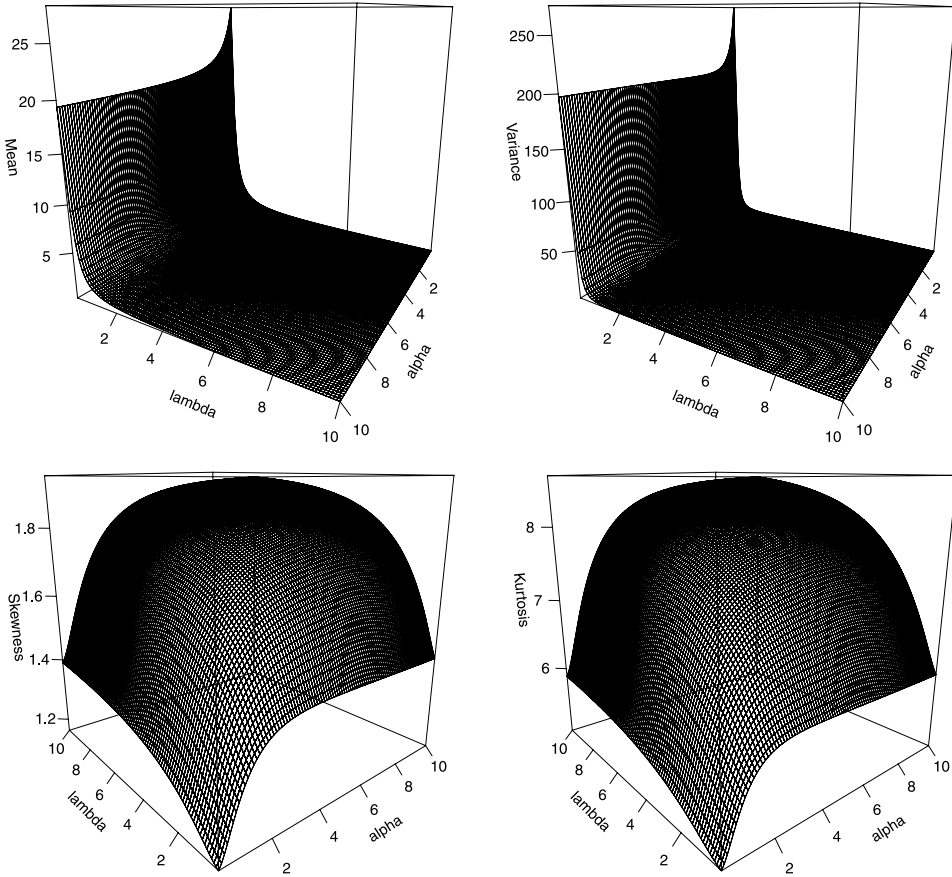


**Figure 3** Mean (top left), variance (top right), skewness (bottom left) and kurtosis (bottom right) of the NWL distribution.

and

$$\begin{aligned} \rho_M^{(2)} = & \log\{[(1 + \alpha)^2(1 + \lambda + \lambda x_p) - e^{-\alpha\lambda x_p}(\lambda(1 + \alpha)(x_p + 1) + 1)] \\ & \times [\alpha p(\lambda(1 + \alpha) + 2 + \alpha)]\} \\ & - \log\{[(1 + \alpha)^2(1 + \lambda + \lambda x_{1-p}) - e^{-\alpha\lambda x_{1-p}}(\lambda(1 + \alpha)(x_{1-p} + 1) + 1)] \\ & \times [\alpha(1 - p)(\lambda(1 + \alpha) + 2 + \alpha)]\}. \end{aligned}$$

Figure 4 plots  $\rho_M$  for some values of the parameters. We can see, again, that the magnitude of skewness increases as both  $\alpha$  and  $\lambda$  increase.

### 3.2 Hazard rate and mean residual life functions

In reliability studies, the hazard rate (failure rate) and mean residual life functions are important characteristics and fundamental to the design of safe systems in a

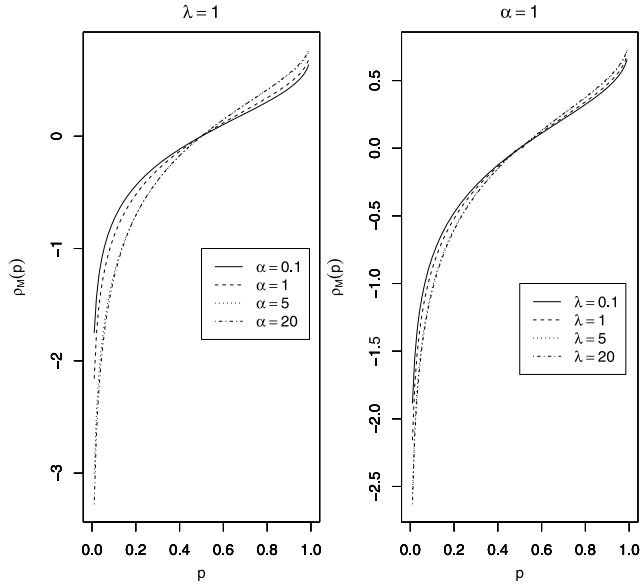


**Figure 4** MacGillivray's skewness function for the NWL distribution.

wide variety of applications. Therefore, we discuss these properties in the case of the NWL distribution.

Based on (9) and (10), the hazard rate function of the NWL distribution is

$$h(x) = \frac{\lambda^2(1+\alpha)^2(1+x)(1-e^{-\alpha\lambda x})}{(1+\alpha)^2(1+\lambda+\lambda x) - [\lambda(1+\alpha)(1+x) + 1]e^{-\alpha\lambda x}}.$$

In particular,  $\lim_{\alpha \rightarrow +\infty} h(x) = \frac{\lambda^2(1+x)}{1+\lambda+\lambda x}$ , the hazard rate function of the Lindley distribution.

The following proposition derives the analytical shape of the hazard rate function.

**Proposition 4.** *The hazard rate function  $h(x)$  is an increasing function for all  $\alpha$  and  $\lambda$ .*

**Proof.** Let  $\eta(x) = -\frac{d \log f(x)}{dx}$ . Since

$$\frac{d\eta(x)}{dx} = \frac{1}{(1+x)^2} + \frac{\alpha^2 \lambda^2 e^{-\alpha\lambda x}}{(1-e^{-\alpha\lambda x})^2} > 0,$$

Glaser's lemma (Glaser, 1980) implies that  $h(x)$  is increasing in  $x$  for all values of  $\alpha$  and  $\lambda$ .  $\square$

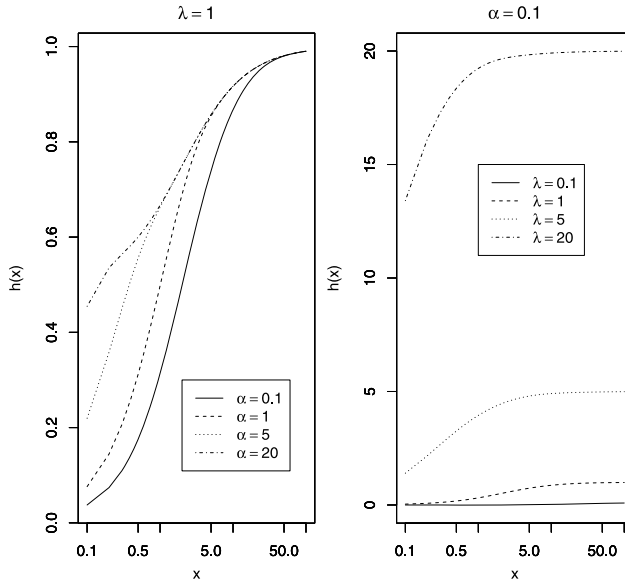


**Figure 5** Hazard rate function of the NWL distribution. The  $x$  axes are in log scale.

**Remark 2.** The hazard rate function is bounded since  $h(0) = 0$  and  $h(+\infty) = \lambda$ . Furthermore,

$$h(x) \sim \frac{\lambda^2(1 + \alpha)^2\alpha\lambda}{(1 + \alpha)^2(1 + \lambda) - \lambda(1 + \alpha) - 1}x$$

as  $x \rightarrow 0$ , a polynomial lower tail.

Figure 5 plots the hazard rate function for different values of  $\alpha$  and  $\lambda$ . As shown by the theory,  $h(x)$  is increasing with  $x$ . The value of  $h(x)$  is increasing with increasing  $\alpha$  (respectively,  $\lambda$ ) for fixed  $\lambda$  (respectively,  $\alpha$ ) and fixed  $x$ .

**Proposition 5.** The mean residual life function  $m(x)$  of the NWL distribution is

$$\begin{aligned} m(x) &= E[X - x | X > x] = \frac{1}{1 - F(x)} \int_x^{+\infty} [1 - F(t)] dt \\ &= \frac{(1 + \alpha)^3(2 + \lambda + \lambda x) - e^{-\alpha\lambda x}[2 + \lambda(1 + \alpha) + \lambda(1 + \alpha)x]}{\lambda(1 + \alpha)\{(1 + \alpha)^2(1 + \lambda + \lambda x) - e^{-\alpha\lambda x}[1 + \lambda(1 + \alpha) + \lambda(1 + \alpha)x]\}}. \end{aligned}$$

**Remarks.**

1. Since the hazard rate function is increasing, the mean residual life function  $m(x)$  is decreasing.

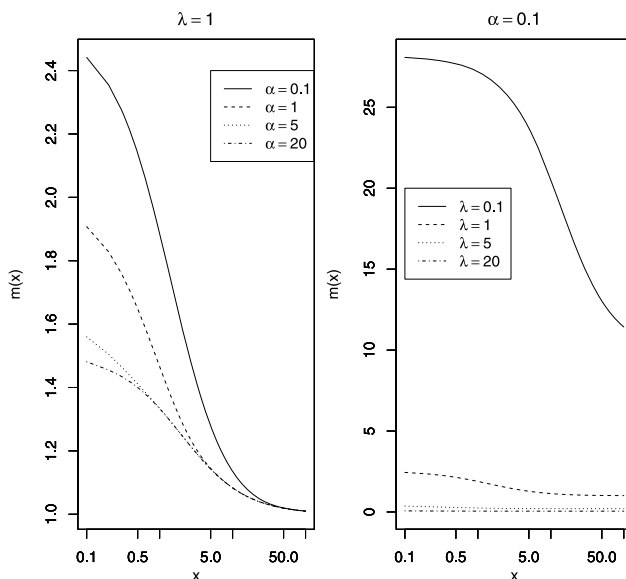


**Figure 6** Mean residual life function of the NWL distribution. The  $x$  axes are in log scale.

2. We have

$$m(0) = \mu = \frac{(1 + \alpha)^3(\lambda + 2) - (1 + \alpha)\lambda - 2}{\lambda(1 + \alpha)[\lambda\alpha(1 + \alpha) + \alpha(2 + \alpha)]} < m(x) < \frac{1}{\lambda} = m(+\infty).$$

3. In the limiting case  $\alpha \rightarrow +\infty$ , we have  $m(x) = \frac{2 + \lambda + \lambda x}{\lambda(1 + \lambda + \lambda x)}$ , the mean residual life function of the Lindley distribution.

Figure 6 plots the mean residual life function for some values of  $\alpha$  and  $\lambda$ . As shown by the theory,  $m(x)$  is decreasing. The value of  $m(x)$  is decreasing with increasing  $\alpha$  (respectively,  $\lambda$ ) for fixed  $\lambda$  (respectively,  $\alpha$ ) and fixed  $x$ .

### 3.3 Lorenz curve, Gini index, Rényi entropy and Mathai–Haubold entropy

The Lorenz curve for a non-negative random variable  $X$  is the graph of

$$L(F(x)) = \frac{\int_0^x tf(t) dt}{\int_0^{+\infty} tf(t) dt}$$

versus  $F(x)$  with the property  $L(p) \leq p$ ,  $L(0) = 0$  and  $L(1) = 1$ . The Gini index of  $X$  is

$$G = 1 - 2 \int_0^1 L(p) dp = 1 - 2 \int_0^{+\infty} L(F(x)) f(x) dx,$$

which can be computed numerically.

Traditionally, applications of the Lorenz curve and the Gini index are in income modeling and related areas, see [Kleiber and Kotz \(2003\)](#). The list of applications is too long to cite. But these concepts have also received applications in other areas: hierarchy theory for digraphs ([Egghe, 2002](#)); depression and cognition ([Maldonado et al., 2007](#)); disease risk to optimize health benefits under cost constraints ([Gail, 2009](#)); seasonal variation of environmental radon gas ([Groves-Kirkby et al., 2009](#)); statistical nonuniformity of sediment transport rate ([Radice, 2009](#)).

**Proposition 6.** *The Lorenz curve of the NWL distribution is*

$$L(p) = \frac{1}{(1 + \alpha)^3(\lambda + 2) - (1 + \alpha)\lambda - 2} \\ \times [e^{-\lambda F^{-1}(p)} \{- (1 + \alpha)^3 [\lambda^2 (F^{-1}(p))^2 + \lambda(\lambda + 2)F^{-1}(p) + (\lambda + 2)] \\ + e^{-\alpha \lambda F^{-1}(p)} [\lambda^2 (1 + \alpha)^2 (F^{-1}(p))^2 \\ + (\lambda(1 + \alpha)(\lambda(1 + \alpha) + 2))F^{-1}(p) \\ + \lambda(1 + \alpha) + 2]\} \\ - 2 + 2(1 + \alpha)^3 - \lambda(1 + \alpha) + \lambda(1 + \alpha)^3].$$

The area between the line  $L(F(x)) = F(x)$  and the Lorenz curve, known as the area of concentration, may be regarded as a measure of inequality of income, so it is important in insurance, economics and other fields like reliability and medicine. Figure 7 shows this area for some values of  $\alpha$  and  $\lambda$ . We see that the area increases as both  $\alpha$  and  $\lambda$  increase. The Lorenz curve is convex by definition (see [Lorenz, 1905](#)), and the curves in Figure 7 appear indeed convex.

The Gini index is a well-known measure for summarizing income inequality. Its range is  $[0, 1]$ . A Gini index of 0 expresses perfect equality, that is every person in the population has an exactly equal income. A Gini index of 1 expresses a maximal inequality, that is only one person has all the income. Figure 8 shows the Gini index for some values of  $\alpha$  and  $\lambda$ . We see that it is increasing as both  $\alpha$  and  $\lambda$  increase. The possible values of the Gini index appear to include at least the interval  $[0.33, 0.45]$ . This range was again determined numerically by computing  $G$  over  $\alpha = 0.01, 0.02, \dots, 100$  and  $\lambda = 0.01, 0.02, \dots, 100$ . We have no analytical proof that  $0.33 \leq G \leq 0.45$ . This is a possible future work.

Entropy is used to measure the randomness of systems and it is widely used in areas like physics, molecular imaging of tumors and sparse kernel density estimation. Two popular entropy measures are the Rényi entropy ([Rényi, 1961](#)) and the Mathai–Haubold entropy ([Mathai and Haubold, 2008](#)) defined by

$$J_R(\gamma) = \frac{1}{1 - \gamma} \log \left\{ \int_{\mathfrak{N}} f^\gamma(x) dx \right\} \quad (12)$$

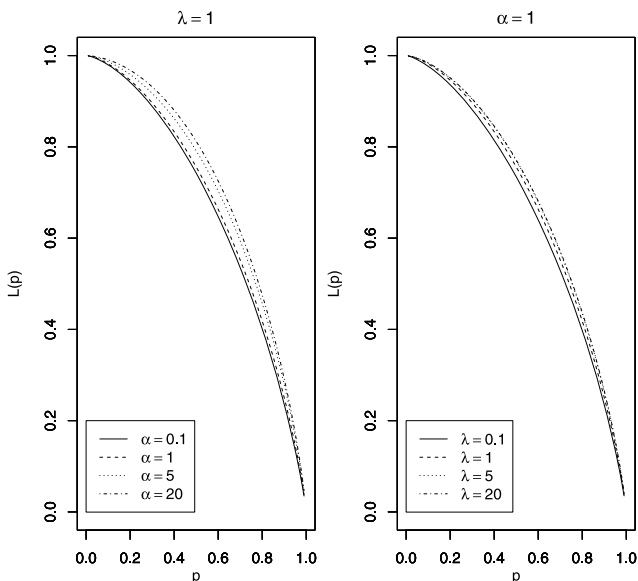


**Figure 7** Lorenz curve of the NWL distribution.

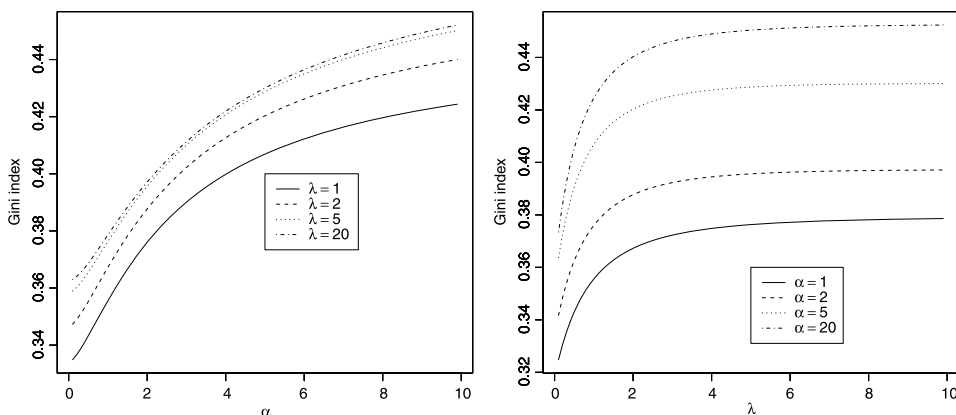


**Figure 8** Gini index of the NWL distribution.

and

$$J_{MH}(\delta) = \frac{\int_{\mathfrak{R}} [f(x)]^{2-\delta} dx - 1}{\delta - 1}, \tag{13}$$

respectively, for  $\gamma > 0$ ,  $\gamma \neq 1$ ,  $\delta \neq 1$  and  $\delta < 2$ . The entropy  $J_{MH}(\delta)$  is an inaccuracy measure through disturbance or distortion of systems.

Some recent applications of the Rényi entropy have been: sparse kernel density estimations (Han et al., 2011); high-resolution scalar quantization (Kreitmeier and

Linder, 2011); estimation of the number of components of a multicomponent non-stationary signal (Sucic et al., 2011); identification of cardiac autonomic neuropathy in diabetes (Jelinek et al., 2012); and signal segmentation in time-frequency plane (Popescu and Aiordachioaie, 2013).

Theorems 1 and 2 derive expressions for these entropies for the NWL distribution.

**Theorem 1.** *The Rényi entropy of the NWL distribution is*

$$J_R(\gamma) = \frac{1}{1-\gamma} \log \left[ \sum_{i=0}^{\infty} \sum_{j=0}^{\infty} \sum_{k=0}^{\infty} \binom{\gamma}{i} \binom{\gamma}{j} \frac{A^\gamma (-1)^{j+k}}{\lambda^{i+1} (\alpha j + \gamma)^{i+1} k! (i+k)} \right]. \quad (14)$$

**Proof.** Using the expansion

$$(1+x)^q = \sum_{i=0}^{\infty} \binom{q}{i} x^i$$

for  $q \in \mathfrak{R}$  and  $|x| < 1$ , we have

$$\begin{aligned} \int_0^{+\infty} f^\gamma(x) dx &= \sum_{i=0}^{\infty} \sum_{j=0}^{\infty} \binom{\gamma}{i} \binom{\gamma}{j} A^\gamma (-1)^j \frac{\delta(i+1, 1)}{\lambda^{i+1} (\alpha j + \gamma)^{i+1}} \\ &= \sum_{i=0}^{\infty} \sum_{j=0}^{\infty} \sum_{k=0}^{\infty} \binom{\gamma}{i} \binom{\gamma}{j} \frac{A^\gamma (-1)^{j+k}}{\lambda^{i+1} (\alpha j + \gamma)^{i+1} k! (i+k)}, \end{aligned}$$

where  $\delta(a, b)$  is the lower incomplete gamma function given by

$$\delta(a, b) = \int_0^b x^{a-1} e^{-x} dx = \sum_{k=0}^{\infty} \frac{(-1)^k b^{a+k}}{k! a + k},$$

and  $A = \frac{\lambda^2(1+\alpha)^2}{\alpha\lambda(1+\alpha)+\alpha(2+\alpha)}$ . The proof is complete.  $\square$

**Theorem 2.** *The Mathai–Haubold entropy of the NWL distribution is*

$$\begin{aligned} J_{MH}(\delta) &= \frac{1}{\delta-1} \\ &\times \left[ \sum_{i=0}^{\infty} \sum_{j=0}^{\infty} \sum_{k=0}^{\infty} \binom{2-\delta}{i} \binom{2-\delta}{j} \frac{A^{2-\delta} (-1)^{j+k}}{\lambda^{i+1} (\alpha j + 2 - \delta)^{i+1} k! (i+k)} - 1 \right]. \quad (15) \end{aligned}$$

**Proof.** Note that

$$\int_0^{\infty} f^{2-\delta}(x) dx = \sum_{i=0}^{\infty} \sum_{j=0}^{\infty} \sum_{k=0}^{\infty} \binom{2-\delta}{i} \binom{2-\delta}{j} \frac{A^{2-\delta} (-1)^{j+k}}{\lambda^{i+1} (\alpha j + 2 - \delta)^{i+1} k! (i+k)}.$$

The proof is complete.  $\square$

Finally, we show how (14) and (16) can be computed in practice. We claim that the infinite series in each of these can be truncated at twenty to yield a high degree of accuracy. In fact, extensive computations showed that the absolute difference between (12) and the truncated version of (14) did not exceed  $10^{-20}$  for all  $\gamma = 0.01, 0.02, \dots, 0.99, 1.01, \dots, 10$ ,  $\alpha = 0.01, 0.02, \dots, 10$ , and  $\lambda = 0.01, 0.02, \dots, 10$ . The absolute difference between (13) and the truncated version of (16) did not exceed  $10^{-20}$  for all  $\delta = 0.01, 0.02, \dots, 0.99, 1.01, \dots, 1.99$ ,  $\alpha = 0.01, 0.02, \dots, 10$ , and  $\lambda = 0.01, 0.02, \dots, 10$ .

## 4 Inference with simulation and data application

In this section, we consider maximum likelihood estimation of the unknown parameters  $\alpha$  and  $\lambda$  of the NWL distribution and give an expression for the associated Fisher's information matrix. Also, simulation results on the behavior of maximum likelihood estimators and a real data application are presented.

### 4.1 Maximum likelihood estimation and information matrix

Let  $x_1, \dots, x_n$  be a random sample of size  $n$  from the NWL distribution. The log-likelihood function is

$$l(\alpha, \lambda) = 2n \log(\lambda) + 2n \log(1 + \alpha) - n \log(\alpha) - n \log[\lambda(1 + \alpha) + 2 + \alpha] \\ + \sum_{i=1}^n \log(1 + x_i) + \sum_{i=1}^n \log(1 - e^{-\alpha\lambda x_i}) - \lambda \sum_{i=1}^n x_i.$$

The maximum likelihood estimators of  $\alpha$  and  $\lambda$  say  $\hat{\alpha}$  and  $\hat{\lambda}$  are the simultaneous solutions of the equations

$$\frac{\partial l(\alpha, \lambda)}{\partial \alpha} = \frac{2n}{1 + \alpha} - \frac{n[\lambda(1 + 2\alpha) + 2(1 + \alpha)]}{\alpha[\lambda(1 + \alpha) + 2 + \alpha]} + \lambda \sum_{i=1}^n \frac{x_i e^{-\alpha\lambda x_i}}{1 - e^{-\alpha\lambda x_i}} = 0,$$

and

$$\frac{\partial l(\alpha, \lambda)}{\partial \lambda} = \frac{2n}{\lambda} - \frac{n(1 + \alpha)}{\lambda(1 + \alpha) + 2 + \alpha} + \alpha \sum_{i=1}^n \frac{x_i e^{-\alpha\lambda x_i}}{1 - e^{-\alpha\lambda x_i}} - \sum_{i=1}^n x_i = 0.$$

For interval estimation and hypothesis testing of the parameters  $\alpha$  and  $\lambda$ , we provide the Fisher information matrix.

**Theorem 3.** *The Fisher information matrix of the maximum likelihood estimators of  $\alpha$  and  $\lambda$  is*

$$I_F(\alpha, \lambda) = - \begin{pmatrix} E(I_{\alpha\alpha}) & E(I_{\alpha\lambda}) \\ E(I_{\lambda\alpha}) & E(I_{\lambda\lambda}) \end{pmatrix},$$

where  $I_{\alpha\alpha} = \frac{\partial^2 l(\alpha, \lambda)}{\partial \alpha^2}$ ,  $I_{\lambda\lambda} = \frac{\partial^2 l(\alpha, \lambda)}{\partial \lambda^2}$  and  $I_{\alpha\lambda} = I_{\lambda\alpha} = \frac{\partial^2 l(\alpha, \lambda)}{\partial \alpha \partial \lambda}$ , and their expectations are given in the [Appendix](#).

**Proof.** The proof uses

$$E\left[\frac{X^2 e^{-\alpha\lambda X}}{(1 - e^{-\alpha\lambda X})^2}\right] = \frac{(1 + \alpha)^2 [\psi'''(1 + 1/\alpha) - \lambda\alpha\psi''(1 + 1/\alpha)]}{\alpha^5 \lambda^2 [\lambda(1 + \alpha) + 2 + \alpha]}$$

and

$$E\left[\frac{X e^{-\alpha\lambda X}}{1 - e^{-\alpha\lambda X}}\right] = \frac{\lambda(1 + \alpha) + 2}{\alpha\lambda(1 + \alpha)[\lambda(1 + \alpha) + 2 + \alpha]},$$

where  $\psi^{(n)}(x)$  denotes the  $n$ th derivative of the digamma function  $\psi(x)$ .  $\square$

**Proposition 7.** Under certain regularity conditions (see, for example, Ferguson, 1996), the distribution of  $\sqrt{n}(\hat{\alpha} - \alpha, \hat{\lambda} - \lambda)$  as  $n \rightarrow +\infty$  is bivariate normal with zero means and variance covariance matrix  $I_F^{-1}(\alpha, \lambda)$ .

**Corollary 2.** Based on Theorem 3,

$$\text{Var}(\hat{\alpha}) \approx \frac{1}{E(I_{\alpha\alpha})}, \quad \text{Cov}(\hat{\alpha}, \hat{\lambda}) = \frac{1}{E(I_{\alpha\lambda})} \neq 0, \quad \text{Var}(\hat{\lambda}) \approx \frac{1}{E(I_{\lambda\lambda})}$$

for large  $n$ . Therefore,  $\hat{\alpha}$  and  $\hat{\lambda}$  are not asymptotically independent.

**Corollary 3.** Based on Theorem 3, the asymptotic confidence intervals for  $\alpha$  and  $\lambda$  with significance level  $\gamma$  are

$$\hat{\alpha} - z_{\gamma/2} \sqrt{\frac{1}{E(I_{\alpha\alpha})}} \Big|_{\alpha=\hat{\alpha}} < \alpha < \hat{\alpha} + z_{\gamma/2} \sqrt{\frac{1}{E(I_{\alpha\alpha})}} \Big|_{\alpha=\hat{\alpha}}$$

and

$$\hat{\lambda} - z_{\gamma/2} \sqrt{\frac{1}{E(I_{\lambda\lambda})}} \Big|_{\lambda=\hat{\lambda}} < \lambda < \hat{\lambda} + z_{\gamma/2} \sqrt{\frac{1}{E(I_{\lambda\lambda})}} \Big|_{\lambda=\hat{\lambda}},$$

respectively, where  $z_a$  denotes the  $100a$  percentile of a standard normal distribution.

## 4.2 Simulation study

Here, we assess the performance of the maximum likelihood estimators  $\hat{\alpha}$  and  $\hat{\lambda}$  with respect to sample size  $n$ . The assessment was based on a simulation study:

1. Generate ten thousand samples of size  $n$  from (9). The inversion method was used to generate samples.
2. Compute the maximum likelihood estimates for the ten thousand samples, say  $(\hat{\alpha}_i, \hat{\lambda}_i)$  for  $i = 1, 2, \dots, 10,000$ .
3. Compute the standard errors of the maximum likelihood estimates for the ten thousand samples, say  $(s_{i,\hat{\alpha}}, s_{i,\hat{\lambda}})$  for  $i = 1, 2, \dots, 10,000$ .

4. Compute the biases, mean squared errors, coverage lengths and coverage probabilities given by

$$\text{bias}_h(n) = \frac{1}{10,000} \sum_{i=1}^{10,000} (\hat{h}_i - h), \quad \text{MSE}_h(n) = \frac{1}{10,000} \sum_{i=1}^{10,000} (\hat{h}_i - h)^2$$

and

$$\text{CL}_h(n) = \frac{2 \cdot 1.959964}{10,000} \sum_{i=1}^{10,000} s_{i,\hat{h}},$$

$$\text{CP}_h(n) = \frac{1}{10,000} \sum_{i=1}^{10,000} I\{\hat{h}_i - 1.959964 \cdot s_{i,\hat{h}} < h < \hat{h}_i + 1.959964 \cdot s_{i,\hat{h}}\}$$

for  $h = \alpha, \lambda$ , where  $I\{\cdot\}$  denotes the indicator function.

We repeated these steps for  $n = 10, 11, \dots, 100$  with  $\alpha = 1$  and  $\lambda = 1$ , so computing  $\text{bias}_h(n)$ ,  $\text{MSE}_h(n)$ ,  $\text{CL}_h(n)$  and  $\text{CP}_h(n)$  for  $h = \alpha, \lambda$  and  $n = 10, 11, \dots, 100$ .

Figures 9, 10, 11 and 12 show how the two biases, the two mean squared errors, the two coverage lengths and the two coverage probabilities vary with respect to  $n$ . Also shown in Figure 10 are the asymptotic mean squared errors computed using Theorem 3. The horizontal lines in Figure 9 correspond to the biases being zero. The horizontal lines in Figure 10 correspond to the mean squared errors being zero. The horizontal lines in Figure 12 correspond to the coverage probabilities being 0.95.

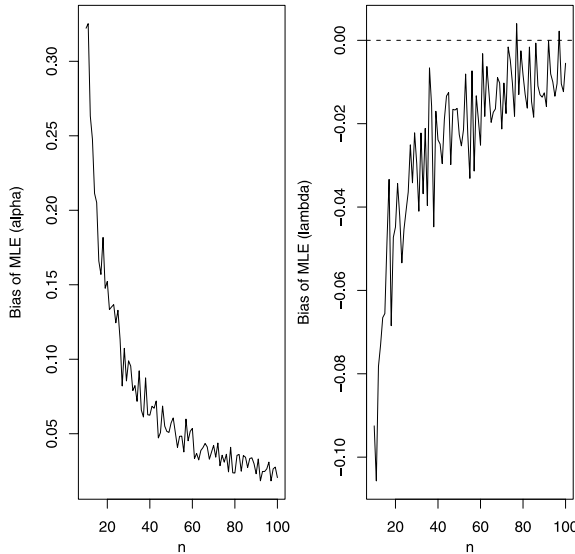


**Figure 9** Biases of  $(\hat{\alpha}, \hat{\lambda})$  versus  $n$ .

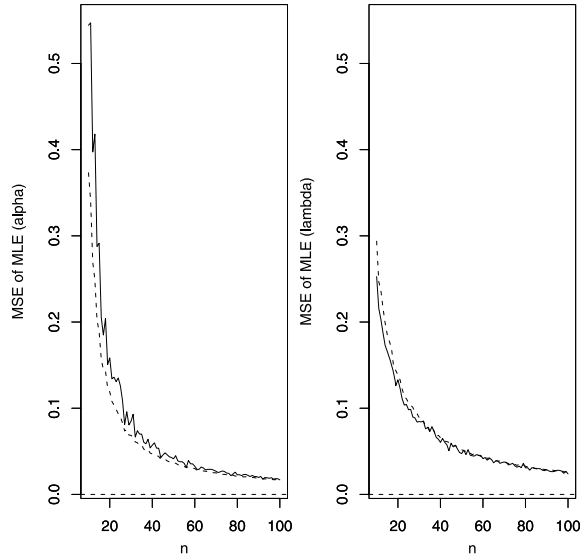


**Figure 10** Mean squared errors (solid) and asymptotic mean squared errors (broken) of  $(\hat{\alpha}, \hat{\lambda})$  versus  $n$ .

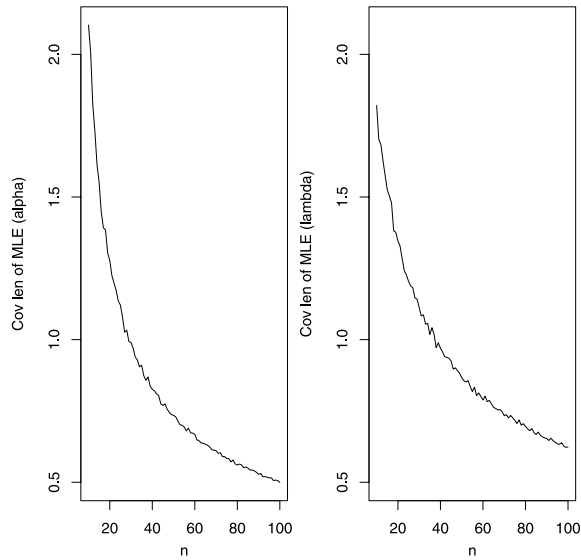


**Figure 11** Coverage lengths of  $(\hat{\alpha}, \hat{\lambda})$  versus  $n$ .

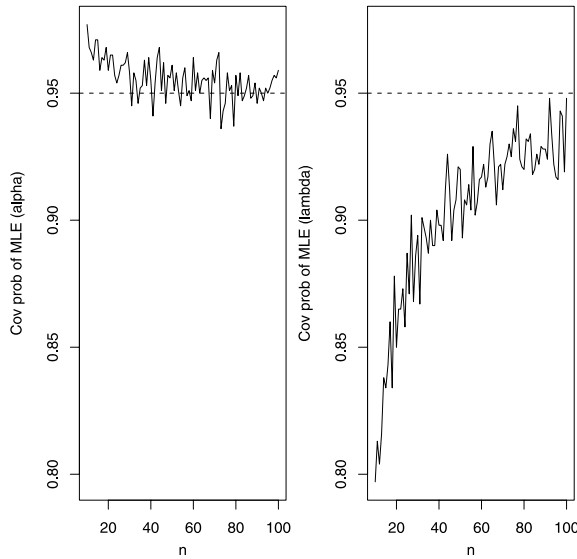


**Figure 12** Coverage probabilities of  $(\hat{\alpha}, \hat{\lambda})$  versus  $n$ .

The following observations can be drawn from the figures: the biases for  $\alpha$  appear generally positive; the biases for  $\lambda$  appear generally negative; the biases for each parameter approach zero with increasing  $n$ ; the biases appear larger for  $\alpha$ ; the biases appear smaller for  $\lambda$ ; the mean squared errors for each parameter decrease to zero with increasing  $n$ ; the mean squared errors appear larger for  $\alpha$ ; the mean squared errors appear smaller for  $\lambda$ ; the asymptotic mean squared errors appear smaller than the mean squared errors for  $\alpha$ ; the asymptotic mean squared errors appear greater than the mean squared errors for  $\lambda$ ; the difference between asymptotic mean squared errors and mean squared errors diminishes with increasing  $n$ ; the coverage lengths for each parameter decrease to zero with increasing  $n$ ; the coverage lengths appear larger for  $\alpha$ ; the coverage lengths appear smaller for  $\lambda$ ; the coverage probabilities for  $\alpha$  appear generally greater than the nominal level; the coverage probabilities for  $\lambda$  appear generally smaller than the nominal level; the coverage probabilities for each parameter approach the nominal level with increasing  $n$ ; the coverage probabilities for  $\alpha$  are generally closer to the nominal level. These observations are for  $\alpha = 1$  and  $\lambda = 1$ . But similar observations were noted for other values of  $\alpha$  and  $\lambda$ .

Section 4.3 presents a real data application. The sample size is thirty eight. We shall see later in Section 4.3 that the NWL distribution provides a good fit to the data set. Based on this fact, the biases for  $\hat{\alpha}$  and  $\hat{\lambda}$  can be expected to be less than 0.05 and 0.02, respectively. The mean squared errors for  $\hat{\alpha}$  and  $\hat{\lambda}$  can be expected to be less than 0.05 and 0.06, respectively. The difference between asymptotic mean squared errors and mean squared errors appears negligible at  $n = 38$ . The coverage lengths for  $\hat{\alpha}$  and  $\hat{\lambda}$  can be expected to be less than 0.8 and 0.9, respectively. The

coverage probabilities for  $\hat{\alpha}$  and  $\hat{\lambda}$  can be expected to be within 0.01 and 0.05 of the nominal level, respectively. Hence, the point estimates given in Section 4.3 can be considered accurate enough.

### 4.3 Data application

Here, we illustrate the power of the NWL distribution by using the carbon data discussed in Section 1.

We fitted the following eleven distributions to the carbon data: the Lindley distribution specified by the p.d.f. (1); the GL distribution specified by the p.d.f. (2); the WEL distribution specified by the p.d.f. (3); the EL distribution specified by the p.d.f. (4); the EPL distribution specified by the p.d.f. (5); the PL distribution specified by the p.d.f. (6); the WL distribution specified by the p.d.f. (7); the GIL distribution specified by the p.d.f. (8); the proposed NWL distribution specified by the p.d.f. (9); the Weibull distribution specified by the p.d.f.

$$f(x) = ab^a x^{a-1} \exp[-(bx)^a]$$

for  $x > 0$ ,  $a > 0$  and  $b > 0$ ; the gamma distribution specified by the p.d.f.

$$f(x) = \frac{b^a}{\Gamma(a)} x^{a-1} \exp(-bx)$$

for  $x > 0$ ,  $a > 0$  and  $b > 0$ . Note that these distributions include all of the known generalizations of the Lindley distribution. The GL, EL and WL distributions have each three parameters. The WEL, EPL, PL, GIL, NWL, Weibull and gamma distributions have each two parameters. The Lindley distribution has one parameter.

Each distribution was fitted by the method of maximum likelihood. The NWL distribution was fitted by following the details in Section 4.1.

Table 1 lists the parameter estimates, their standard errors (computed by inverting the observed information matrices), the negative log-likelihood values, the values of the Akaike information criterion (AIC), the values of the Bayesian information criterion (BIC), the  $p$ -values based on the Kolmogorov–Smirnov statistic and the  $p$ -values based on the test due to [Chen and Balakrishnan \(1995\)](#).

We see that the NWL distribution has the largest log-likelihood value, the smallest AIC value, the smallest BIC value, the largest  $p$ -value based on the Kolmogorov–Smirnov test, and the largest  $p$ -value based on [Chen and Balakrishnan's \(1995\)](#) test in spite of the fact that three of the fitted distributions have more parameters. The WEL and gamma distributions have the second largest log-likelihood value, the second smallest AIC value, the second smallest BIC value, the second largest  $p$ -value based on the Kolmogorov–Smirnov test, and the sec-

**Table 1** Parameter estimates, standard errors, log-likelihood values and goodness of fit measures

Distribution	Estimates (ses)	Log-likelihood	AIC	BIC	KS $p$ -value	CB $p$ -value
Lindley	$\hat{\lambda} = 3.438 \times 10^{-4}$ ( $5.025 \times 10^{-5}$ )	358.98	719.95	721.59	0.45	0.4
NWL	$\hat{\alpha} = 1.000$ (1.788), $\hat{\lambda} = 4.009 \times 10^{-4}$ ( $1.355 \times 10^{-4}$ )	356.86	717.72	721.00	0.72	0.70
EL	$\hat{\lambda} = 9.824 \times 10^{-1}$ ( $4.414 \times 10^{-1}$ ), $\hat{\alpha} = -5.264 \times 10^{-7}$ ( $2.376 \times 10^{-7}$ ), $\hat{\beta} = 9.029 \times 10^{-2}$ ( $9.934 \times 10^{-3}$ )	467.167	940.33	945.25	0.02	0.01
WEL	$\hat{\theta} = 5.461 \times 10^{-4}$ ( $7.227 \times 10^{-4}$ ), $\hat{c} = 2.172$ (3.294)	357.02	718.04	721.32	0.61	0.58
EPL	$\hat{\theta} = 2.679 \times 10^4$ ( $2.004 \times 10^3$ ), $\hat{\beta} = 1.717 \times 10^{-4}$ ( $8.492 \times 10^{-5}$ )	367.35	738.70	741.97	0.04	0.04
GL	$\hat{\theta} = 2.817 \times 10^{-2}$ ( $1.422 \times 10^{-2}$ ), $\hat{\alpha} = 2.239 \times 10^{-6}$ ( $3.307 \times 10^{-1}$ ), $\hat{\gamma} = 3.495 \times 10^{-2}$ ( $9.228 \times 10^{-3}$ )	6376.23	12,758.46	12,763.38	0.01	0.01
PL	$\hat{\alpha} = 1.202$ (1.045), $\hat{\beta} = 5.712 \times 10^{-5}$ ( $4.671 \times 10^{-5}$ )	357.77	719.53	722.81	0.59	0.55
WL	$\hat{\lambda} = 3.894 \times 10^{-4}$ ( $3.065 \times 10^{-5}$ ), $\hat{\alpha} = 7.709 \times 10^{-1}$ ( $5.201 \times 10^{-2}$ ), $\hat{\beta} = 3.981 \times 10^{-7}$ ( $6.956 \times 10^{-9}$ )	359.71	725.42	730.37	0.05	0.05
Weibull	$\hat{a} = 1.670$ ( $7.454 \times 10^{-1}$ ), $\hat{b} = 1.526 \times 10^{-4}$ ( $9.937 \times 10^{-5}$ )	359.75	723.50	726.77	0.11	0.09
Gamma	$\hat{a} = 3.171$ ( $6.936 \times 10^{-1}$ ), $\hat{b} = 1.831 \times 10^3$ ( $4.340 \times 10^2$ )	357.02	718.04	721.32	0.61	0.60
GIL	$\hat{\alpha} = 1.148$ ( $5.986 \times 10^{-2}$ ), $\hat{\lambda} = 1.262 \times 10^4$ ( $5.863 \times 10^3$ )	363.85	731.71	734.98	0.04	0.03

ond largest  $p$ -value based on [Chen and Balakrishnan's \(1995\)](#) test. The GL distribution has the smallest log-likelihood value, the largest AIC value, the largest BIC value, the smallest  $p$ -value based on the Kolmogorov–Smirnov test, and the smallest  $p$ -value based on [Chen and Balakrishnan's \(1995\)](#) test. The EL distribution has the second smallest log-likelihood value, the second largest AIC value, the second largest BIC value, the second smallest  $p$ -value based on the Kolmogorov–Smirnov test, and the second smallest  $p$ -value based on [Chen and Balakrishnan's \(1995\)](#) test.

Thus we can conclude that the NWL distribution provides the best fit among the distributions considered here for the carbon data. The second best fit is by the WEL and gamma distributions. The worst fit is by the GL distribution. The second worst fit is by the EL distribution. The density and probability plots shown in [Figures 13 and 14](#) confirm these observations. The fitted p.d.f. of the NWL distribution best captures the empirical histogram. The plotted points for the NWL distribution are most closest to the diagonal line in the probability plot.

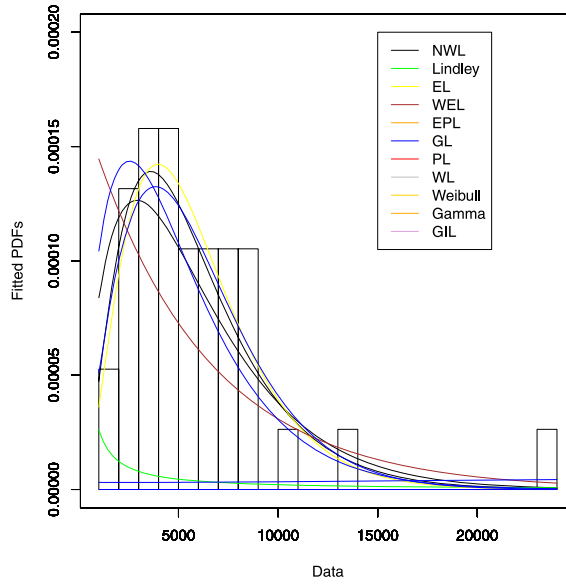


**Figure 13** Histogram of the carbon data and the fitted p.d.f.s of the Lindley, GL, WEL, EL, EPL, PL, WL, GIL, NWL, Weibull and gamma distributions.

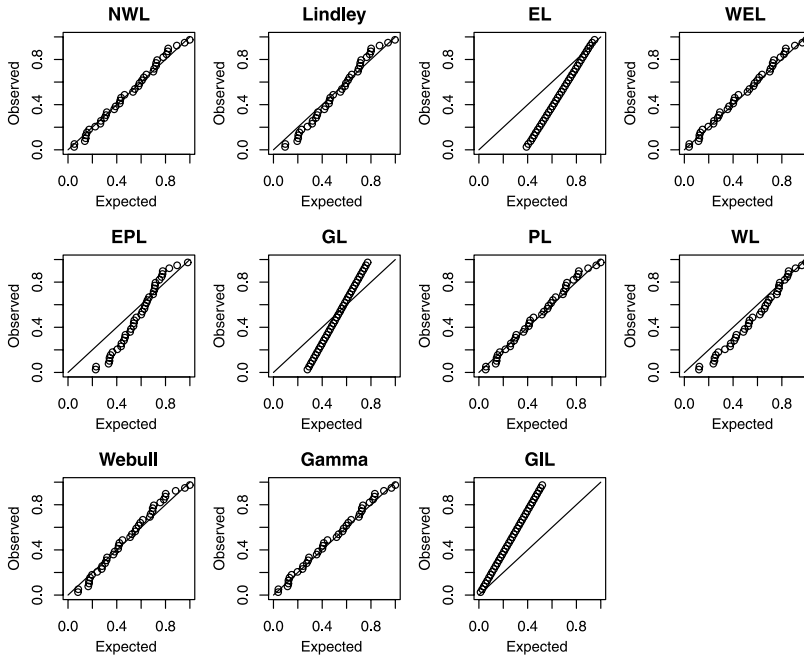


**Figure 14** Probability plots for the fits of the Lindley, GL, WEL, EL, EPL, PL, WL, GIL, NWL, Weibull and gamma distributions.

## Appendix

Here, we provide the elements of the Fisher's information matrix  $I_F(\alpha, \lambda)$ . They are

$$\begin{aligned}
 I_{\alpha\alpha} &= \frac{\partial^2 l(\alpha, \lambda)}{\partial \alpha^2} \\
 &= -\frac{2n}{(1+\alpha)^2} \\
 &\quad + n \frac{(1+2\alpha+2\alpha^2)\lambda^2 + 2(2+3\alpha+2\alpha^2)\lambda + 2(2+2\alpha+\alpha^2)}{\alpha^2[\lambda(1+\alpha) + 2 + \alpha]^2} \\
 &\quad - \lambda^2 \sum_{i=1}^n \frac{x_i^2 e^{-\alpha\lambda x_i}}{(1 - e^{-\alpha\lambda x_i})^2}, \\
 I_{\lambda\lambda} &= \frac{\partial^2 l(\alpha, \lambda)}{\partial \lambda^2} = -\frac{2n}{\lambda^2} + \frac{n(1+\alpha)^2}{[\lambda(1+\alpha) + 2 + \alpha]^2} - \alpha^2 \sum_{i=1}^n \frac{x_i^2 e^{-\alpha\lambda x_i}}{(1 - e^{-\alpha\lambda x_i})^2},
 \end{aligned}$$

$$\begin{aligned}
 I_{\alpha\lambda} &= I_{\lambda\alpha} = \frac{\partial^2 l(\alpha, \lambda)}{\partial \alpha \partial \lambda} \\
 &= -\frac{n}{[\lambda(1+\alpha) + 2 + \alpha]^2} + \sum_{i=1}^n \frac{x_i e^{-\alpha\lambda x_i}}{1 - e^{-\alpha\lambda x_i}} - \lambda\alpha \sum_{i=1}^n \frac{x_i^2 e^{-\alpha\lambda x_i}}{(1 - e^{-\alpha\lambda x_i})^2},
 \end{aligned}$$

$$\begin{aligned}
 E(I_{\alpha\alpha}) &= -\frac{2n}{(1+\alpha)^2} \\
 &\quad + n \frac{(1+2\alpha+2\alpha^2)\lambda^2 + 2(2+3\alpha+2\alpha^2)\lambda + 2(2+2\alpha+\alpha^2)}{\alpha^2[\lambda(1+\alpha) + 2 + \alpha]^2} \\
 &\quad - n \frac{(1+\alpha)^2[\psi'''(1+1/\alpha) - \lambda\alpha\psi''(1+1/\alpha)]}{\alpha^5[\lambda(1+\alpha) + 2 + \alpha]},
 \end{aligned}$$

$$\begin{aligned}
 E(I_{\lambda\lambda}) &= -\frac{2n}{\lambda^2} + \frac{n(1+\alpha)^2}{[\lambda(1+\alpha) + 2 + \alpha]^2} \\
 &\quad - n \frac{(1+\alpha)^2[\psi'''(1+1/\alpha) - \lambda\alpha\psi''(1+1/\alpha)]}{\alpha^3\lambda^2[\lambda(1+\alpha) + 2 + \alpha]}
 \end{aligned}$$

and

$$\begin{aligned}
 E(I_{\alpha\lambda}) &= -\frac{n}{[\lambda(1+\alpha) + 2 + \alpha]^2} + \frac{n[\lambda(1+\alpha) + 2]}{\alpha\lambda(1+\alpha)[\lambda(1+\alpha) + (2+\alpha)]} \\
 &\quad - \frac{n(1+\alpha)^2[\psi'''(1+1/\alpha) - \lambda\alpha\psi''(1+1/\alpha)]}{\alpha^4\lambda[\lambda(1+\alpha) + 2 + \alpha]}.
 \end{aligned}$$

## Acknowledgments

The authors would like to thank the Editor, the Associate Editor and the two referees for careful reading and for their comments which greatly improved the paper.

## References

- Asai, N., Kubo, I. and Kuo, H. H. (2001). Roles of log-concavity, log-convexity, and growth order in white noise analysis. *Infinite Dimensional Analysis Quantum Probability and Related Topics* **4**, 59–84. [MR1824473](#)
- Asgharzadeh, A., Nadarajah, S. and Sharafi, F. (2014a). Generalized inverse Lindley distribution. Preprint.
- Asgharzadeh, A., Sharafi, F. and Nadarajah, S. (2014b). Weibull Lindley distribution. Preprint.
- Azzalini, A. (1985). A class of distributions which includes the normal ones. *Scandinavian Journal of Statistics* **12**, 171–178. [MR0808153](#)
- Bakouch, H. S., Al-Zahrani, B. M., Al-Shomrani, A. A., Marchi, V. A. A. and Louzada, F. (2012). An extended Lindley distribution. *Journal of the Korean Statistical Society* **41**, 75–85. [MR2933216](#)
- Barreto-Souza, W. and Bakouch, H. S. (2013). A new lifetime model with decreasing failure rate. *Statistics* **47**, 465–476. [MR3043713](#)
- Chen, G. and Balakrishnan, N. (1995). A general purpose approximate goodness-of-fit test. *Journal of Quality Technology* **27**, 154–161.
- Egghe, L. (2002). Development of hierarchy theory for digraphs using concentration theory based on a new type of Lorenz curve. *Mathematical and Computer Modelling* **36**, 587–602. [MR1928609](#)
- Ferguson, T. S. (1996). *A Course in Large Sample Theory*. London: Chapman & Hall. [MR1699953](#)
- Gail, M. H. (2009). Applying the Lorenz curve to disease risk to optimize health benefits under cost constraints. *Statistics and Its Interface* **2**, 117–121. [MR2516062](#)
- Ghitany, M. E., Al-Mutairi, D. K., Balakrishnan, N. and Al-Enezi, L. J. (2013). Power Lindley distribution and associated inference. *Computational Statistics and Data Analysis* **64**, 20–33. [MR3061887](#)
- Ghitany, M. E., Alqallaf, F., Al-Mutairi, D. K. and Husain, H. A. (2011). A two-parameter weighted Lindley distribution and its applications to survival data. *Mathematics and Computers in Simulation* **81**, 1190–1201. [MR2769828](#)
- Ghitany, M. E., Atieh, B. and Nadarajah, S. (2008). Lindley distribution and its application. *Mathematics and Computers in Simulation* **78**, 493–506. [MR2424558](#)
- Glaser, R. E. (1980). Bathtub and related failure rate characterizations. *Journal of the American Statistical Association* **75**, 667–672. [MR0590699](#)
- Groves-Kirkby, C. J., Denman, A. R. and Phillips, P. S. (2009). Lorenz curve and Gini coefficient: Novel tools for analysing seasonal variation of environmental radon gas. *Journal of Environmental Management* **90**, 2480–2487.
- Gupta, R. D. and Kundu, D. (2009). A new class of weighted exponential distributions. *Statistics* **43**, 621–634. [MR2588273](#)
- Han, M., Liang, Z. and Li, D. (2011). Sparse kernel density estimations and its application in variable selection based on quadratic Renyi entropy. *Neurocomputing* **74**, 1664–1672.
- Jelinek, H. F., Tarvainen, M. P. and Cornforth, D. J. (2012). Renyi entropy in identification of cardiac autonomic neuropathy in diabetes. In *Proceedings of the 39th Conference on Computing in Cardiology* 909–911. Krakow: IEEE.
- Kleiber, C. and Kotz, S. (2003). *Statistical Size Distributions in Economics and Actuarial Sciences*. New York: Wiley. [MR1994050](#)

- Koutras, V. P. (2011). Two-level software rejuvenation model with increasing failure rate degradation. In *Dependable Computer Systems* 101–115. New York: Springer.
- Kreitmeyer, W. and Linder, T. (2011). High-resolution scalar quantization with Renyi entropy constraint. *IEEE Transactions on Information Theory* **57**, 6837–6859. [MR2882266](#)
- Lai, M.-T. (2013). Optimum number of minimal repairs for a system under increasing failure rate shock model with cumulative repair-cost limit. *International Journal of Reliability and Safety* **7**, 95–107.
- Lindley, D. V. (1958). Fiducial distributions and Bayes' theorem. *Journal of the Royal Statistical Society, Ser. B* **20**, 102–107. [MR0095550](#)
- Lorenz, M. O. (1905). Methods of measuring the concentration of wealth. *Publications of the American Statistical Association* **9**, 209–219.
- MacGillivray, H. L. (1986). Skewness and asymmetry: Measures and orderings. *The Annals of Statistics* **14**, 994–1011. [MR0856802](#)
- Maeda, K. and Nishikawa, M. (2006). Duration of party control in parliamentary and presidential governments: A study of 65 democracies, 1950 to 1998. *Comparative Political Studies* **39**, 352–374.
- Maldonado, A., Perez-Ocon, R. and Herrera, A. (2007). Depression and cognition: New insights from the Lorenz curve and the Gini index. *International Journal of Clinical and Health Psychology* **7**, 21–39.
- Mathai, A. M. and Haubold, H. J. (2008). On generalized distributions and pathways. *Physics Letters A* **372**, 2109–2113.
- Milkie, C. M. and Perakis, A. N. (2004). Statistical methods for planning diesel engine overhauls in the U.S. coast guard. *Naval Engineers Journal* 31–41.
- Nadarajah, S. (2009). The skew logistic distribution. *Advances in Statistical Analysis* **93**, 197–203. [MR2511595](#)
- Ninh, A. and Prekopa, A. (2013). Log-concavity of compound distributions with applications in stochastic optimization. *Discrete Applied Mathematics* **161**, 3017–3027. [MR3126668](#)
- Popescu, T. D. and Aiordachioaie, D. (2013). Signal segmentation in time-frequency plane using Renyi entropy—Application in seismic signal processing. In *Proceedings of the Second International Conference on Control and Fault-Tolerant Systems* 312–317. Nice, France: IEEE.
- Radice, A. (2009). Use of the Lorenz curve to quantify statistical nonuniformity of sediment transport rate. *Journal of Hydraulic Engineering* **135**, 320–326.
- Rényi, A. (1961). On measures of entropy and information. In *Proceedings of the 4th Berkeley Symposium on Mathematical Statistics and Probability, Vol. I* 547–561. Berkeley: Univ. California Press. [MR0132570](#)
- Saidane, S., Babai, M. Z., Aguir, M. S. and Korbaa, O. (2011). Spare parts inventory systems under an increasing failure rate demand interval distribution. In *Proceedings of the 41st International Conference on Computers and Industrial Engineering* 768–773. Los Angeles, CA.
- Shakhathreh, M. K. (2012). A two-parameter of weighted exponential distributions. *Statistics and Probability Letters* **82**, 252–261. [MR2875208](#)
- Sucic, V., Saulig, N. and Boashash, B. (2011). Estimating the number of components of a multi-component nonstationary signal using the short-term time-frequency Renyi entropy. *EURASIP Journal on Advances in Signal Processing* **2011**, 125.
- Tsarouhas, P. H. and Arvanitoyannis, I. S. (2010). Reliability and maintainability analysis of bread production line. *Critical Reviews in Food Science and Nutrition* **50**, 327–343.
- Ugarte, M. D., Militino, A. F. and Arnholt, A. T. (2008). *Probability and Statistics with R*. London: Chapman & Hall. [MR2404651](#)
- Woolsey, R. L. and Cossman, J. (2007). Drug development and the FDA's critical path initiative. *Clinical Pharmacology and Therapeutics* **81**, 129–133.

Zakerzadeh, H. and Dolati, A. (2009). Generalized Lindley distribution. *Journal of Mathematical Extension* **3**, 13–25. MR2985582

A. Asgharzadeh  
F. Sharafi  
Department of Statistics  
University of Mazandaran  
P.O. Box 47416-1467  
Babolsar  
Iran  
E-mail: [a.asgharzadeh@umz.ac.ir](mailto:a.asgharzadeh@umz.ac.ir)  
[fatemeh\\_sharafi@yahoo.com](mailto:fatemeh_sharafi@yahoo.com)

Hassan S. Backouch  
Mathematics Department  
Faculty of Science  
Tanta University  
Tanta  
Egypt  
and  
Water Research Center  
King Abdulaziz University  
Jeddah 21589  
Saudi Arabia  
E-mail: [hnbakouch@yahoo.com](mailto:hnbakouch@yahoo.com)

S. Nadarajah  
School of Mathematics  
University of Manchester  
Manchester, M13 9PL  
United Kingdom  
E-mail: [mbbssn2@manchester.ac.uk](mailto:mbbssn2@manchester.ac.uk)